World Academy of Science, Engineering and Technology
International Journal of Mechanical and Mechatronics Engineering
Vol:9, No:2, 2015

Prediction and Reduction of Cracking Issue in Precision Forging of Engine Valves Using Finite Element Method

Xi Yang, Bulent Chavdar, Alan Vonseggern, Taylan Altan

***Abstract*—**Fracture in hot precision forging of engine valves was investigated in this paper. The entire valve forging procedure was described and the possible cause of the fracture was proposed. Finite Element simulation was conducted for the forging process, with commercial Finite Element code DEFORM^{TM}. The effects of material properties, the effect of strain rate and temperature were considered in the FE simulation. Two fracture criteria were discussed and compared, based on the accuracy and reliability of the FE simulation results. The selected criterion predicted the fracture location and shows the trend of damage increasing with good accuracy, which matches the experimental observation. Additional modification of the punch shapes was proposed to further reduce the tendency of fracture in forging. Finite Element comparison shows a great potential of such application in the mass production.

***Keywords*—**Hot forging, engine valve, fracture, tooling.

I. Introduction

FRACTURE in forging is a lengthy and difficult problem, which many researchers have spent decades try to solve. Ductile fracture of the material generally goes through a progressive deterioration process, namely void nucleation, growth and coalescence. A term - forgeability (forming limit) of a metal - can be defined as its capability to undergo deformation by forging without cracking. Considerable fracture theories which based on different aspects, such as continuum mechanics, material grain boundary evolution, etc. were developed.

Reference [1] roughly divided the fracture models into three categories:

1) Fracture mechanics model (FM): this model takes the integral of the plastic work over the strain history. Once the damage value reaches a critical value, which is the threshold of the material failure, fracture initiates. Example: [2]-[6].
2) Micro-based damage mechanics model (MDM): this model is derived from analysis on isolated unit cells involving idealized defects such as cracks, voids, or second phase particles. Example: [7]-[9].
3) Meso-based mechanics model (CDM): this model implies that at increasing level of material damage, the material resistance to deformation decreases, since the effective resistant area reduces. Example: [10]-[16]

Generally, many fracture criteria could predict ductile fracture initiation in cold working with good accuracy. References [17], [18] made a comprehensive study by comparing different FM fracture criteria in predicting ductile fracture in cold working. Reference [19] used FM criteria to predict fracture in various applications such as radial extrusion and open die forging, and concluded that in tri-axial and tension-compression state of stress, the fracture can be predicted successfully. References [20]-[25] used either standard Lemaitre's model or modified enhanced Lemaitre's model to predict ductile fracture in different cold working applications.

The study in application of fracture criteria in hot working is relatively limited. In hot forging, the complex situation where strain rate and temperature effects are involved makes the fracture prediction extremely challenging.

References [26], [27] used Lemaitre's model to predict fracture in warm forming of complicated parts such as journal bearings and hexagon socket screw. They proved that with enough material parameters measurements and proper calibration, method of effective stress could predict the fracture in warm forging with great accuracy.

Reference [28] conducted a study of the cavitation and failure during hot compression of Ti-6Al-4V. The depth of crack and the cavitation was measured and compared with FE simulations using C&L and Rice&Tracey fracture model. The conclusion is the fracture model could capture the location of the fracture precisely. Also, it could predict the depth of the cracking approximately.

Reference [29] conducted a study to compare the capability of many fracture criteria using cylinder compression test and collar test. After determining the critical values of different criteria, the variation was compared for different models. An ideal fracture criterion should have the critical damage value that is only material dependent. In other words, the critical damage value should be a constant in different forging conditions. However, the measured critical values for all the damage model studies showed variation for different forging conditions. The C&L, method of effective stress and maximum principle stress/UTS exhibit a relative constant critical damage value.

Based on the literature search, very few studies applied the fracture model to reduce the fracture issue in an actual hot forging process. In this study, the fracture formation in hot

X. Y. is with the General Motors-Powertrain, Pontiac, MI 48340 USA (corresponding author to provide phone: 614-620-3002; e-mail: xi.yang@gm.com).

B. C. is with the Eaton Corporation, Corporate Research and Technology Center, Southfield, MI 48076 (e-mail: BulentChavdar@eaton.com).

A. V.S. is with the Eaton Corporation, Vehicle Group, Kearney, NE 68847, USA.

T. A. is with the Center for Precision Forming, The Ohio State University, Columbus, OH 43210, USA (e-mail: altan.1@osu.edu).

precision forging of the mass produced engine valves was investigated. The fracture initiation was predicted using selected fracture criteria and the alternative tooling design was proposed to reduce the fracture in a mass production line.

II. Problem Statement

The precision forging of engine valves is a well-established procedure that has been utilized by many manufacturers. A common manufacturing procedure includes the following steps: 1) billet shearing and heating; 2) extrusion to obtain an "onion" shape preform; 3) coining to form the valve head. Fig. 1 shows the forging procedure schematically [30].

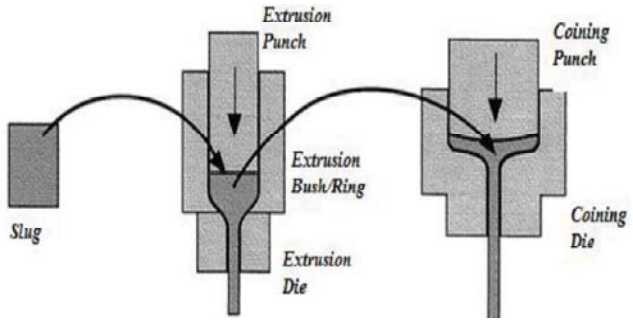

Fig. 1 Valve forging schematic [30]

Fig. 2 Cracks at the "blade" area after coining

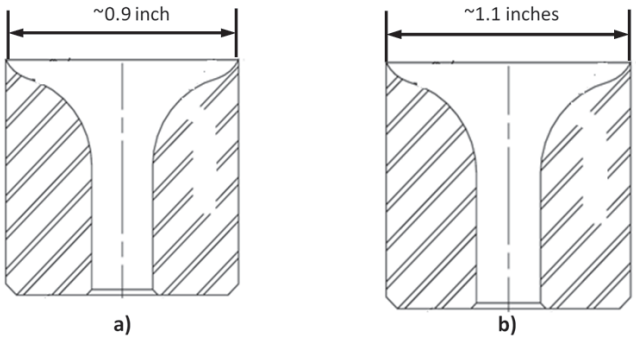

Fig. 3 (a) extrusion die with smaller diameter; (b) extrusion die with larger diameter

In order to improve the high temperature corrosion resistance and increase the part life in the severe operating environment of the combustion engine, high Chrome-Nickel based stainless steel 23-8N is introduced to replace the previous 21-2N as the valve material. However, due to the high percentage of the Chrome and Nickel addition, the formability of the steel at elevated temperature decreases. As a result, the material is likely to fracture during the forging operation. Experiment has shown that if the new material (23-8N) is processed with the previous die set and procedure, which is designed to form 21-2N, the material is likely to crack during coining. Fracture is observed at the "blade" (periphery) area, at the top of the valve head, as indicated in Fig. 2.

Another experimental observation is, if the billet is extruded in the extrusion die with a larger diameter (Fig. 3 (b)) and then coined in the same coining die, cracking can be reduced.

III. Methodology

A. Fracture Criterion

In order to understand the fracture formation, the forging process of both extrusion and coining needs to be simulated using finite element method to emulate the material behavior. A suitable fracture criterion has to be selected to predict the cracking during hot forging. According to [29], Cockcroft and Latham, maximum principle stress/UTS and method of effective stress could be the suitable fracture models to emulate hot forging process. Typically, method of effective stress requires certain calibration procedure to determine the material's constant. Thus, the method of effective stress will be investigated in the future work. In current study, the other two fracture criteria - Cockcroft and Latham, maximum principle stress/UTS were utilized to estimate the fracture formation.

Maximum principle stress/UTS criterion:

$$C = \frac{\sigma^*_{max}}{UTS(T,\dot{\bar{\varepsilon}})} \quad (1)$$

where C = instantaneous damage value; σ^*_{max} = maximum principle stress; UTS = ultimate tensile strength; T = temperature; $\dot{\bar{\varepsilon}}$ = strain rate; Cockcroft and Latham criterion:

$$C = \int_0^{\bar{\varepsilon}} \left(\frac{\sigma^*_{max}}{\bar{\sigma}}\right) d\bar{\varepsilon} \quad (2)$$

where C = instantaneous damage value; σ^*_{max} = maximum principle stress; $\bar{\sigma}$ = effective stress; $\bar{\varepsilon}$ = effective strain.

In both of these criteria, a damage value C is defined, which is an instantaneous value that changes with stress-strain state. A larger damage value indicates the material is more likely to crack. If we can find a critical damage value Ccritical for the specific material and forging conditions by experiment, we can predict the moment when cracking occurs, i.e. once the instantaneous damage value is larger than the critical value, the material will crack. Typically, the exact critical damage value is very difficult to determine.

B. Material Properties

Table I shows the material's properties of 23-8N obtained from Eaton Corp. The forging temperature of 23-8N is 1120°C - 1170°C. The highest temperature available from the data

sheet is 870°C. To estimate the material's behavior at elevated temperature till about 1200°C, the properties (thermal expansion, thermal conductivity, UTS, yield stress, etc.) have to be extrapolated from the available data.

TABLE I
MATERIAL PROPERTIES OF 23-8N (EATON CORP)

Temp (°C)	RT	430	540	650	760	870
Thermal Expansion (ppm/°C)	15.7	17.6	18	18.4	18.8	19.2
Thermal Conductivity (W/cm K)	0.13	0.2	0.2	0.237	0.25	
UTS (MPa)	959	696	629	545	405	228
0.2% YS (MPa)	538	324	290	276	239	159
Elongation (%)	21	27	21	33	36	26
RA (%)	20	27	28	38	44	71
Elastic Modulus (GPa)	206			153	144	

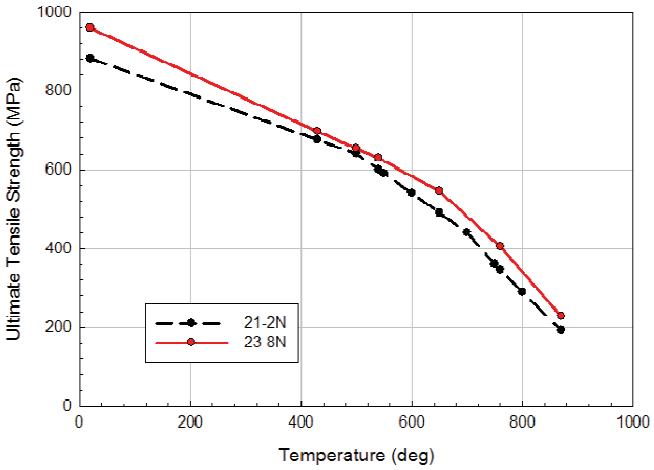

Fig. 4 Ultimate tensile strength of 23-8N and 21-2N at elevated temperature

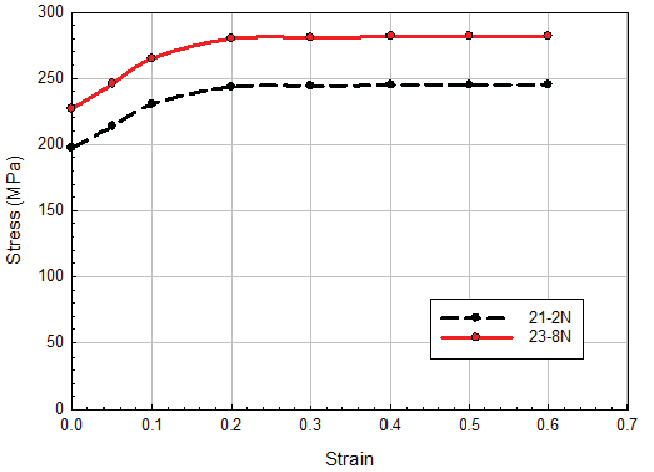

Fig. 5 Flow stress of 23-8N and 21-2N at 1037°C, the strain rate is 2.5s-1

To conduct the finite element simulation, the flow stress of the material at elevated temperature (or at least within the forging temperature range) has to be input to the FE software. However, these data are not available for 23-8N. To estimate the flow stress of this material, another stainless steel, 21-2N, whose flow stress data and other properties are available in the commercial software DEFORM database, was used as a reference. The chemical composition of 23-8N and 21-2N are similar, while 23-8N has slightly higher percentage of Nickel (8%) and Chromium (23%), compared to 21-2N (2% Nickel and 21% Chromium). A higher percentage of Nickel and Chromium composition in 23-8N will result in a higher ultimate tensile strength and flow stress. The ultimate tensile strength of both materials plotted in Fig. 4 illustrates this assumption. It can be seen from the plot that when the temperature is higher 600°C, the ratio of the UTS (23-8N to 21-2N) is almost constant (≈1.2). Since the forging process is conducted at a much higher temperature (≈1150°C); the small variation at lower temperature can be ignored. We then assumed that the flow stress of two materials follows the same ratio at elevated temperature, that is the flow stress of 23-8N is 1.2 times larger than 21-2N. Since the flow stress of 21-2N is available, flow stress of 23-8N at elevated temperature can be estimated. Fig. 5 plots the flow stress of 21-2N and 23-8N at 1037°C as an example.

C. Finite Element Simulation Procedure

Finite element method was used to simulate the extrusion operation with both small and large extrusion dies and the following coining operation. The simulations were conducted with a commercial FE code DEFORM2D. Table II is the summary of the important simulation parameters used in this study.

TABLE II
SIMULATION PARAMETERS

Billet material	23-8N
Flow stress	DEFORM database with modification
Billet temperature	1150°C
Heat transfer coefficient	15kW/m^{2}K
friction (shear factor)	0.3

After extrusion simulation, the "onion" shaped valve preform from the large die has a larger diameter and smaller thickness "head", while the one from the smaller die has a smaller diameter "head" but the thickness is larger. Then in the coining simulation, the two different shaped valve preform were forged in the same coining die. The shape of the extruded and coined part was illustrated in Fig. 6.

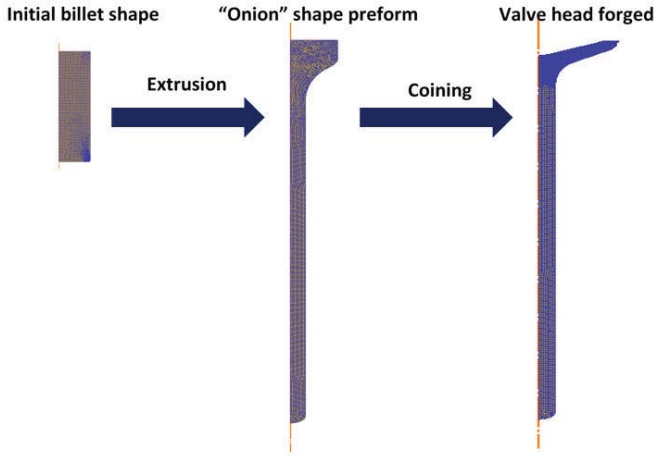

Fig. 6 FE simulation procedure of the extrusion and coining operation

IV. FE Simulation Results and Discussion

It is observed from the fractured samples (Fig. 2) that the cracks only originated from the top surface of the valve head. This indicates that the fracture initiated at the very late stage of the forging operation, when the stroke is near the bottom dead center (BDC) and before the top and bottom die touches each other. In the precision forging die design, flash is added to prevent the extremely high die stress concentration. Thus, the maximum damage values just before the flash is formed (assumed at such moment fracture initiates) were extracted from the simulations and plotted in Figs. 7 and 8.

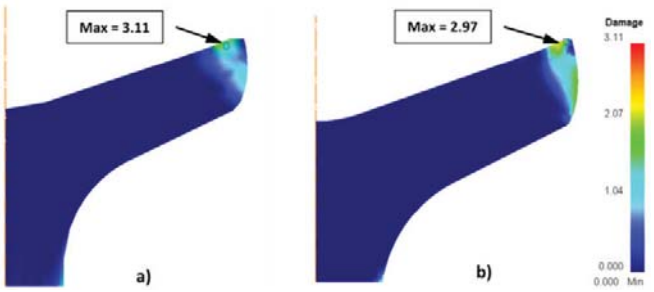

Fig. 7 Maximum damage values with maximum principle stress/UTS criterion: (a) smaller extrusion die; (b) larger extrusion

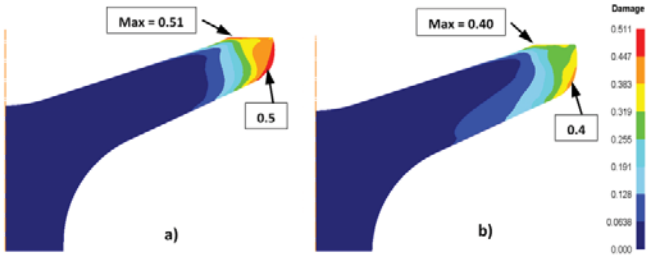

Fig. 8 Maximum damage values with Cockcroft and Latham (C&L) criterion: (a) smaller extrusion die; (b larger extrusion die

It can be seen from the results that both fracture criteria predicted the maximum damage value occurs at the top surface of the part, which matches the experimental observation very well. However, C&L criterion predicted another location which has the same damage level. This results agree with the study conducted by Semiatin [28], which indicates that the maximum pain damage occurs at the maximum bulge radius area. This is because C&L criterion calculates the integral of the plastic deformation over strain history. The maximum bulge radius area is generally another area where strain is the maximum. By carefully observing the fractured samples, it is noticed that the fracture is aligned along the radial direction of the valve head. This is the evidence that the fracture is formed due to the tensile stress in circumferential direction. So, the maximum principle stress and the hoop stress distribution were also plotted for both cases, Figs. 9 and 10. It shows that the maximum principle stress and hoop stress at top surface are much larger than the side of the part. This indicates that the part will crack at the top surface of the valve.

The strain rate comparison in also supports the damage prediction. Since the punch speed is almost Zero when it gets close to the BDC, the strain rate distribution is very similar for the two cases. In both cases, the maximum strain rate occurs at two locations: the top surface and the side of the part, which matches the maximum damage area predicted by C&L criterion. This is because in hot forging, the flow stress of the material is sensitive to strain rate. The flow stress value will be higher if the material undergoes higher strain rate, resulting in higher damage values.

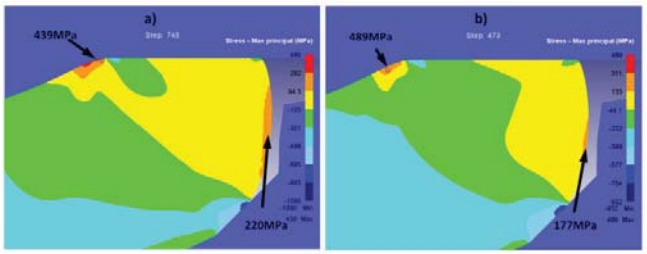

Fig. 9 Maximum principle stress distribution: (a) smaller extrusion die; (b) larger extrusion die (Die stroke: 253.8mm/Total stroke:254mm)

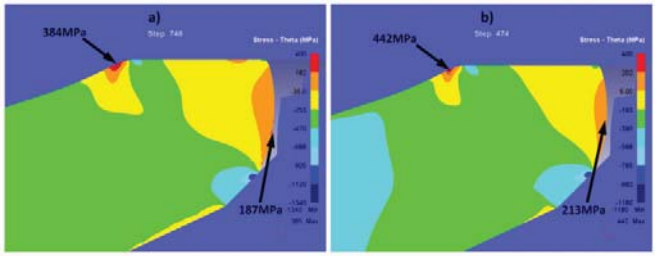

Fig. 10 Hoop stress distribution: (a) smaller extrusion die; (b) larger extrusion die (Die stroke: 253.8mm/Total stroke: 254mm)

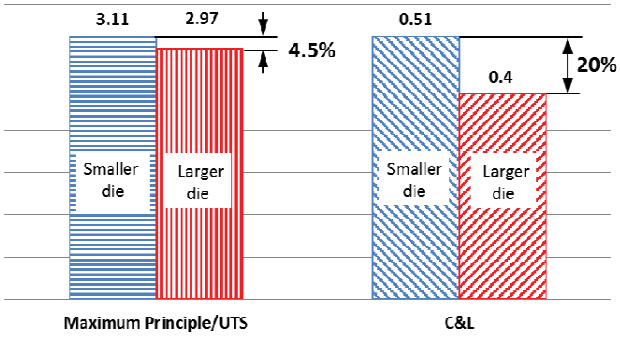

Fig. 11 Maximum damage values predicted with two different fracture criteria

By comparing the results in Figs. 7 and 8, both fracture criteria calculated smaller damage values when a larger extrusion die is used, which means the material is less likely to crack. In another word, both fracture criteria have a good estimation of the fracture initiation potential in hot forging of engine valves.

Fig. 11 plotted the maximum damage values predicted from FEM with different fracture models. It can be seen that the maximum principle stress/UTS criterion estimated 4.5% decrease in the damage value calculation when a large extrusion die is used. Considering the simulation errors, the extrapolation of the UTS values at forging temperature (as explained in Section III) and some other variables in the actual test, such trivial difference is not a strong argument to back up that the fracture is less likely to occur. So in the next section, we selected C&L criterion as our primary model to emulate fracture behavior.

V. Modified Punch Design for Fracture Reduction

To further reduce the risk of cracking, some modified extrusion punch shapes were proposed. One solution is to add a convex bump at the top of the extrusion punch. The protrusion can be either like Figs. 12 (a) or (b), which were named as "convex" punch or "half convex" punch. The extruded preforms with the punch shape are shown in Figs. 13 (a) and (b). The idea behind this is to further reduce the material's deformation during the coining process to lower the cracking risk, since the "onion" head is forged into a shape closer to the end shape of the valve head. Another proposed idea is to use a half concave extrusion punch (Fig. 12 (c)), and the shape of the extruded preform is shown in Fig. 13 (c). The reason for this design is that at the starting point of the coining operation, the coining punch will first touch the apex of the preform head. Then the material in the head area will be forced to flow toward the outside to increase diameter by itself, instead of squeezed by the coining punch.

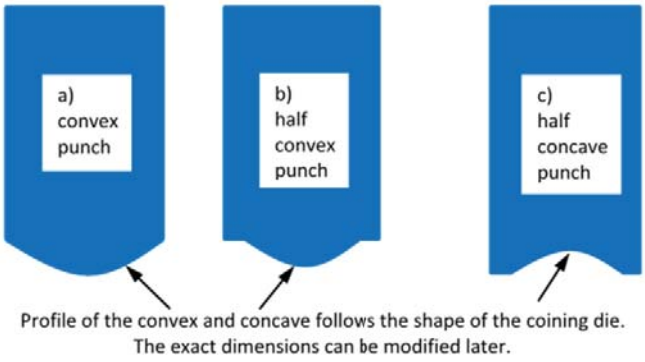

Fig. 12 Schematic of the modified punch shapes (a) convex punch; (b) half convex punch; (c) concave punch

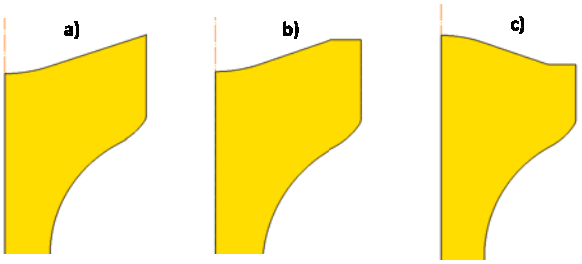

Fig. 13 The shape of the preforms extruded with modified punches: (a) convex punch; (b) half convex punch; (c) concave punch

Extrusion simulation with the modified punch shapes were conducted for both larger extrusion die and smaller extrusion die. The actual punch diameter was adjusted according to the diameter of the extrusion die. Then, the extruded preform with different head shapes were coined in the same coining die. The maximum damage values with C&L criterion were plotted in Fig. 14. Some conclusions can be made by comparing the results from FE simulations.

1) The larger extrusion die will still result in smaller damage values in average, which means the part is less likely to crack if extrude with larger die. Therefore, a larger extrusion die is the optimized option to avoid cracking.
2) Convex punch actually increases the damage values, which indicates the part is more likely to crack. The sharp corner of the preform head might contribute to the damage increase.
3) Half convex punch is the optimized punch shape to lower the cracking risk. The maximum damage value it produces with smaller extrusion die is less than that with flat punch. In the case of larger extrusion die, the damage values are the same with flat and half convex punch. This is because the diameter of the die has more significant influence on the material flow than the punch shape. Also, the profile of the punch shape is not optimized. More iteration steps are necessary in order to optimize the punch convex profile to reduce the damage risk further.
4) For the concave punch concept, the damage values actually increased, which is the opposite result of our assumption. This indicates that the part extruded with concave punch design will be in more danger to fracture.

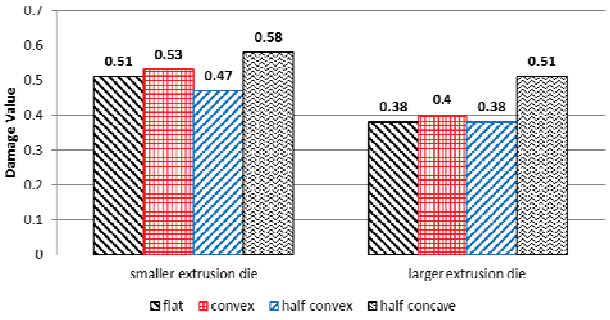

Fig. 14 Maximum Damage Values with Different Punch Designs

VI. Conclusions

1) The valve cracking phenomenon can be estimated using finite element method with the help of suitable fracture criterion. Based on the literature search, two fracture criteria, maximum principle stress/UTS and C&L were selected to estimate the fracture in hot forging.
2) Both fracture criteria predicted a decreased damage value when a larger diameter extrusion die is used. The results agree with the experimental observation that a larger extrusion die could reduce the fracture of the material.
3) Both fracture criteria predicted the correct fracture location. However for C&L criterion, the maximum principle stress or hoop stress distribution is also required to estimate the fraction location.
4) Due to the trivial variation of the damage values produced by maximum principle stress/UTS criterion, C&L criterion was used to the optimization study in hot forging punch shape design.
5) Half convex punch shape in extrusion can further decrease the maximum damage values in coining, which means such design could help to reduce the cracking of the material in actual forging operation. The convex profile requires further optimization in order to be used the actual production line.
6) The convex punch shape will produce a high damage value due to the sharp corner generated on the preform.
7) The concave punch shape will result in much higher damage values, which means it will increase the danger of cracking.

Acknowledgments

This research was conducted as part of the studies funded under the Cooperative Agreement, DE-FG36-08GO18131, awarded by the United States Department of Energy, and led by Eaton Corporation as the prime contractor and the Ohio State University as the subcontractor. The authors are grateful for the experimentation provided by Eaton Forging Plant in Kearney, Nebraska and the discussions provided by Mr. Marcin Czernek at Eaton Forging Plant in Bielsko-Biala, Poland and the support by the Center for Precision Forging at the Ohio State University.

Disclaimer

References

[1] Soyarslan, C., A. E. Tekkaya, et al. (2008). "Application of Continuum Damage Mechanics in discontinuous crack formation: Forward extrusion chevron predictions." Zamm 88(6): 436-453.
[2] Freudenthal, A. M. (1950). The Inelastic Behavior in Solids. New York, Wiley.
[3] Cockcroft, M. G. and D. J. Latham (1968). "Ductility and the workability of metals." Journal of the Institute of Metals 96: 33-39.
[4] Rice, J. R. and D. M. Tracey (1969). "On the ductile enlargement of voids in triaxial stress fields." Journal of the Mechanics and Physics of Solids 17: 201-217.
[5] Brozzo, P., B. Deluca, et al. (1972). A new method for the prediction of formability limits in metal sheets, sheet metal forming and formability. Proceedings of the Seventh Biannual Conference of the International Deep Drawing Research Group.
[6] Oyane, M. (1972). "Criteria of ductile fracture strain." Bull. JSME 15: 1507-1513.
[7] Gurson, A. L. (1977). "Continuum theorie of ductile rupture by void nucleation and growth: Part I. Yield criteria and flow rules for porous ductile media." Journal of Engineering Materials and Technology Transactions ASME 99: 2-15.
[8] Rousselier, G. (1987). "Ductile fracture models and their potential in local approach of fracture." Nuclear Engineering and Design 105: 97-111.
[9] Nahshon, K. and J. W. Hutchinson (2008). "Modification of the Gurson Model for shear failure." European Journal of Mechanics - A/Solids 27: 1-17.
[10] Lemaitre, J. (1971). Evaluation of dissipation and damage in metals. Proceedings of I.C.M. 1.
[11] Steinmann, P., C. Miehe, et al. (1994). "Comparison of different finite deformation inelastic damage models within multiplicative elastoplasticity for ductile material." Computational Mechanics 13: 458-474.
[12] Lammer, H. and C. Tsakmakis (2000). "Discussion of coupled elastoplasticity and damage constitutive equations for small and finite deformations." International Journal of Plasticity 16: 496-523.
[13] Menzel, A. and P. Steinmann (2001). "A theoretical and computational framework for anisotropic continuum damage mechanics at large strains." International Journal of Solids and Structures 38: 9505-9523.
[14] Voyiadjis, G. Z., R. K. A. Al-Rub, et al. (2004). "Thermodynamic formulations for non-local coupling of viscoplasticity and anisotropic viscodamage for dynamic localization problems using gradient theory." International Journal of Plasticity 20: 981-1038.
[15] Brunig, M. and S. Ricci (2005). "Nonlocal continuum theory of anisotropically damaged metals." International Journal of Plasticity 21: 1346-1382.
[16] Mediavilla, J., R. H. J. Peerlings, et al. (2006). "A nonlocal triaxiality-dependent ductile damage model for finite strain plasticity." Computer Methods in Applied Mechanics and Engineering 195: 4317-4634.

[17] CLIFT, S. E., P. HARTLEY, et al. (1990). "Fracture prediction in plastic deformation processes." international Journal of Mechanical Sciences 32(1): 1-17.
[18] Kim, H., M. Yamanaka, et al. (1995). "Prediction And Elimination Of Ductile Fracture In Cold Forgings Using Fem Simulations." Transactions of NAMRI/SME XXIII (63-69).
[19] Gouveia, B. P. P. A., J. M. C. Rodrigues, et al. (2000). "Ductile fracture in metalworking: experimental and theoretical research." Journal of Materials Processing Technology 101(1–3): 52-63.
[20] de Souza Neto, E. A. (2002). "A fast, one-equation integration algorithm for the Lemaitre ductile damage model." Communications in Numerical Methods in Engineering 18(8): 541-554.
[21] Andrade Pires, F. M., J. M. A. César de Sá, et al. (2003). "Numerical modelling of ductile plastic damage in bulk metal forming." International Journal of Mechanical Sciences 45(2): 273-294.
[22] Gupta, S., N. VenkataReddy, et al. (2003). "Ductile fracture prediction in axisymmetric upsetting using continuum damage mechanics." Journal of Materials Processing Technology 141(2): 256-265.
[23] Mashayekhi, M. and S. Ziaei-Rad (2006). "Identification and validation of a ductile damage model for A533 steel." Journal of Materials Processing Technology 177(1-3): 291-295.
[24] Bouchard, P.-O., L. Bourgeon, et al. (2010). "An enhanced Lemaitre model formulation for materials processing damage computation." International Journal of Material Forming 4(3): 299-315.
[25] HajiAboutalebi, F., M. Farzin, et al. (2010). "Numerical simulation and experimental validation of a ductile damage model for DIN 1623 St14 steel." The International Journal of Advanced Manufacturing Technology 53(1-4): 157-165.
[26] Behrens, A. and H. Just (2002). "Extension of the forming limits in cold and warm forging by the FE based fracture analysis with the integrated damage model of effective stresses." Journal of Materials Processing Technology 125–126(0): 235-241.
[27] Behrens, A. and H. Just (2002). "Verification of the damage model of effective stresses in cold and warm forging operations by experimental testing and FE simulations." Journal of Materials Processing Technology 125–126(0): 295-301.
[28] Semiatin, S. L., R. L. Goetz, et al. (1999). "Cavitation and failure during hot forging Ti-6Al-4V." Metallurgical And Materials Transactions A 30A: 1411-1424.
[29] Ruf, G., C. Sommitsch, et al. (2006). Modelling ductile damage of a Ni-base alloy considering the microstructure evolution during hot working. Steel Grips. 1.
[30] Painter, B., R. Shivpuri, et al. (1995). Computer Aided Techniques for the Prediction of Die Wear during Hot Forging of Automotive Exhaust Valves, The Ohio State University.